NON-CONTACT RESPIRATORY RATE ESTIMATION BASED ON RF SIGNALS WITH MACHINE LEARNING ALGORITHMS

Master's Thesis

Ufuk KİRAZCI

Eskişehir 2024

NON-CONTACT RESPIRATORY RATE ESTIMATION BASED ON RF SIGNALS WITH MACHINE LEARNING ALGORITHMS

Ufuk KİRAZCI

Master's Thesis

Department of Electrical and Electronic Engineering

Programme in Telecommunication

Supervisor: Asst. Prof. Dr. Can UYSAL

Eskişehir

Eskişehir Technical University

Institute of Graduate Programs

November 2024

FINAL APPROVAL FOR THESIS

This thesis titled NON-CONTACT RESPIRATORY RATE ESTIMATION BASED ON RF SIGNALS WITH MACHINE LEARNING ALGORITHMS has been prepared and submitted by Ufuk KİRAZCI in partial fulfillment of the requirements in "Eskişehir Technical University Directive on Graduate Education and Examination" for the Degree of Master's in Electrical and Electronic Engineering Department has been examined and approved on 13/11/2024.

Committee Members		**Title, Name and Surname**	**Signature**
Member	:	Asst. Prof. Dr. Can UYSAL	
Member	:	Prof. Dr. Tansu FİLİK	
Member	:	Assoc. Prof. Dr. Erol SEKE	

Prof. Dr. Semra KURAMA
Director of the Institute of Graduate Programs

13/11/2024

SUPERVISOR APPROVAL

Master's student Ufuk KİRAZCI, whom I supervise, has completed this thesis titled NON-CONTACT RESPIRATORY RATE ESTIMATION BASED ON RF SIGNALS WITH MACHINE LEARNING ALGORITHMS. According to my inspections, the work is scientifically and ethically appropriate for the student to the thesis defense exam.

Supervisor
Asst. Prof. Dr. Can UYSAL

ABSTRACT

NON-CONTACT RESPIRATORY RATE ESTIMATION BASED ON RF SIGNALS WITH MACHINE LEARNING ALGORITHMS

Ufuk KİRAZCI

Department of Electrical and Electronic Engineering

Programme in Telecommunication

Eskişehir Technical University, Institute of Graduate Programs, November 2024

Supervisor: Asst. Prof. Dr. Can UYSAL

Respiratory rate is a very important parameter in the field of health monitoring. In any clinical or emergency medical situation, monitoring the patient's respiratory rate is one of the one of the critical first examinations to understand the general condition of the patient and to determine the intervention to be performed. Researchers continue to work on developing a highly accurate respiratory rate estimation method within limited observation period. In this study, we propose a new non-contact respiratory rate estimation method using radio-frequency (RF) signals and machine learning models within a limited observation time. 10 different people's respiratory data are used in this study, and software-based radios are used to generate and receive RF signals. The performances of various machine learning models on the dataset are extracted and the model that gives the best result is used. Experimental results show that the proposed method achieves an error rate of 2.33% for a limited observation time of 10 seconds and is superior to the existing methods in the literature.

Keywords: Non-Contact, Respiratory rate estimation, Health monitoring, RF signals, Machine learning.

ÖZET

MAKİNE ÖĞRENME ALGORİTMALARI İLE RF SİNYALLERİNE DAYALI TEMASSIZ SOLUNUM HIZI TAHMİNİ

Ufuk KİRAZCI

Elektrik - Elektronik Mühendisliği Anabilim Dalı

Telekomünikasyon Bilim Dalı

Eskişehir Teknik Üniversitesi, Lisansüstü Eğitim Enstitüsü, Kasım 2024

Danışman: Dr. Öğr. Üyesi Can UYSAL

Solunum hızı, sağlık izleme alanında oldukça önemli bir parametre durumundadır. Herhangi bir klinik ya da acil tıbbi durumda hastanın solunum hızını izleme, hastanın genel durumunu anlamak ve yapılacak müdahaleyi belirlemek için kritik ilk muayenelerden birisidir. Araştırmacılar, sınırlı gözlem süresi içerisinde, yüksek doğruluklu solunum hızı kestirim methodu geliştirmek için çalışmalar yapmaya devam etmektedir. Bu çalışmada, radyo-frekans (RF) sinyalleri kullanılarak makine öğrenmesi modelleri ile sınırlı gözlem süresi içerisinde, temassız solunum hızı kestirimi yapabilen yeni bir yöntem önerilmektedir. 10 farklı kişinin solunum verilerinin kullanıldığı bu çalışmada, RF sinyallerini üretmek ve almak için yazılım tabanlı radyolar kullanılmaktadır. Veri seti üzerinde çeşitli makine öğrenmesi modellerinin performansları çıkarılarak en iyi sonucu veren model kullanılmaktadır. Önerilen yöntemin, 10 saniye gibi sınırlı gözlem süresi için %2.33 hata oranına ulaştığı ve literatürdeki mevcut yöntemlerden daha üstün olduğu deneysel sonuçlarla gösterilmektedir.

Anahtar Sözcükler: Temassız, Solunum hızı kestirimi, Sağlık izleme, RF sinyaller, Makine öğrenmesi.

ACKNOWLEDGEMENTS

I would like to express my endless thanks to my supervisor Asst. Prof. Dr. Can UYSAL for his support, always encouraging me and never leaving any of my questions unanswered.

I would like to thank my esteemed professors in the thesis defense committee for their interest.

I would like to thank my family for their support throughout my education life.

I would like to thank my beloved wife for always believing in me.

Ufuk KİRAZCI

13/11/2024

STATEMENT OF COMPLIANCE WITH ETHICAL PRINCIPLES AND RULES

I hereby truthfully declare that this thesis is an original work prepared by me; that I have behaved in accordance with the scientific ethical principles and rules throughout the stages of preparation, data collection, analysis and presentation of my work; that I have cited the sources of all the data and information that could be obtained within the scope of this study, and included these sources in the references section; and that this study has been scanned for plagiarism with "scientific plagiarism detection program" used by Eskişehir Technical University, and that "it does not have any plagiarism" whatsoever. I also declare that, if a case contrary to my declaration is detected in my work at any time, I hereby express my consent to all the ethical and legal consequences that are involved.

Ufuk KİRAZCI

CONTENTS

Page

LIST OF TABLES

Page

LIST OF FIGURES

Page

GLOSSARY OF SYMBOLS AND ABBREVIATIONS

BPM	:	Breathe Per Minute
CSI	:	Channel State Information
ECG	:	Electrocardiography
FFT	:	Fast Fourier Transform
FMCW	:	Frequency Modulated Continuous Wave
IF	:	Intermediate Frequency
MAPE	:	Mean Absolute Percentage Error
ML	:	Machine Learning
MLP	:	Multilayer Perceptron
PSG	:	Polysomnography
PPG	:	Photoplethysmography
RF	:	Radio Frequency
RQI	:	Respiratory Quality Index
RR	:	Respiratory Rate
SpO2	:	Oxygen Saturation
SDR	:	Software Defined Radio
St. Dev	:	Standard Deviation

1. INTRODUCTION

In this section, the subject of the study, its importance in literature and the proposed method are mentioned.

1.1. Overview

Like heart rate, oxygen saturation, blood pressure and body temperature, respiratory rate (RR) is an important indicator that provides vital information about a person's health status [1,2]. Vital signs usually serve as the first step of every medical evaluation or examination. There are many studies in the literature showing that respiratory rate can be used as important data for early disease detection, monitoring sleep quality and monitoring the status and development of existing diseases such as severe acute respiratory syndrome (SARS) and COVID-19 [3,4,5,6]. In addition, Nicolo et al. pointed out the importance of RR monitoring and presented sensors and techniques suitable for monitoring RR in specific disease scenarios such as various stressors including emotional stress, cognitive load, hyperthermia and others [2].

In recent years, many studies have been conducted showing the importance of respiratory rate monitoring by researchers. Wuerich et al. showed that the urgency status of the patient can be determined by measuring the RR at the hospital entrance with a non-contact video based model in their 2021 study [6]. In another study, Natarajan et al. showed that longitudinal changes in nocturnal RR can be a valuable biometric in the detection and monitoring of COVID-19 [7]. Similarly, Uysal et al. suggested that the use of elderly surveillance systems that can monitor the RR of the elderly and people in need of care in the home environment in a non-contact way to be informed their vital activities has become widespread in recent years [8].

In conclusion, high accuracy RR estimation is an important issue that is greatly of interest to researchers today. In addition, in terms of measurement methods used in RR estimation, non-contact methods look bright since they provide comfort, accessibility, confidentiality and convenience to the user.

Figure 1.1 shows a real-time display of vital signals. These vital signs are heart rate, blood pressure, O2 saturation and respiration rate.

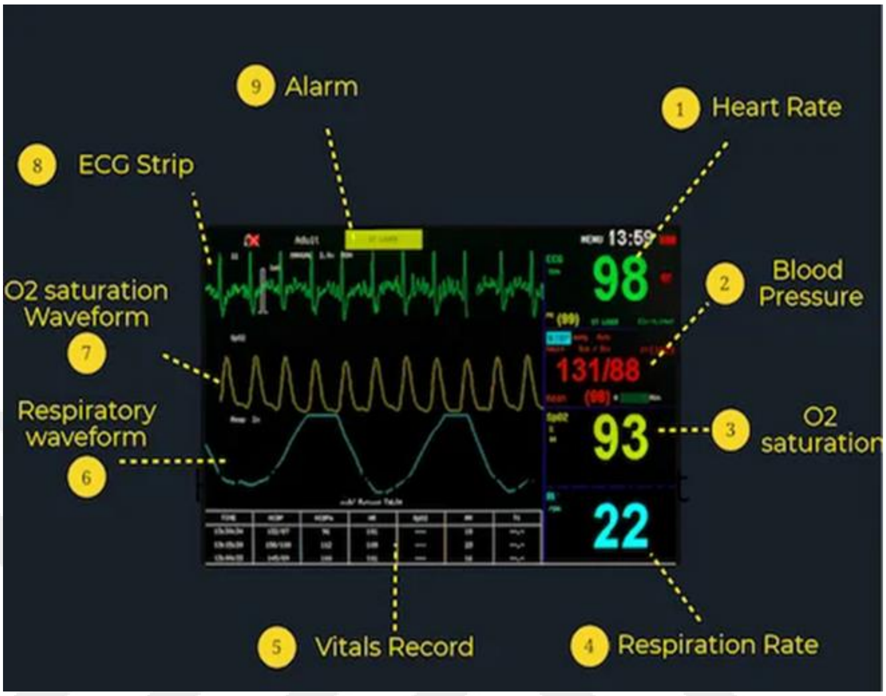

Figure 1.1. *Vital signs in the health monitoring area.*

1.2. Goals and Motivation

In this study, RR estimation is performed with various machine learning algorithms in a non-contact manner using RF signals with SDR modules. Existing methods in the literature can estimate respiratory rate with high accuracy for larger observation periods (such as one minute), while their accuracies decrease when the observation period decreases (10 seconds). This is an important problem for applications in clinical settings and especially emergency scenarios. In this study, a machine learning based method is proposed to overcome this challenge. The proposed method can estimate respiration rate with high accuracy in a limited observation time of 10 seconds.

2. RELATED WORKS

In the first part of this chapter, previously proposed methods in the literature for contact and non-contact respiration rate estimation are reviewed. The subject of this study is RR estimation with machine learning algorithms using RF signals and the studies conducted with this method in the literature are also analysed in the second part of the chapter.

2.1. Overview

RR estimation has become very popular in recent years due to the increasing importance of health monitoring. RR can be estimated by various methods in literature. These methods are basically divided into two as contact based or non-contact based. There are many studies in the literature that have been carried out in both ways. Traditionally, RR is estimated by commercial wearable devices containing sensors such as electrocardiography (ECG) [9,10], polysomnography (PSG), photoplethysmography (PPG) [10,11,12,13]. Several recent studies have investigated the use of PPG and ECG signals to obtain RR with a wearable device. In a study conducted in 2021, a RQI scheme has been developed to improve the performance of neural networks utilizing the respiratory modulations of ECG and PPG signals for RR estimation [10]. In another study, Shuzan et al. proposed a novel method for estimating the RR and oxygen saturation (SpO2) from photoplethysmogram signals [14]. Despite the disadvantages such as increasing the workload of the staff, disturbing comfort and restricting the daily movements of the person, studies using contact-based sensors continue today thanks to their advantages such as high accuracy and less sensitivity to external factors [14,15,16].

In recent years, a number of studies have been carried out on RR measurement with non-contact based sensors as an alternative to contact-based sensors. Basically, non-contact methods attract the interest of researchers to eliminate the disadvantages of contact-based systems, especially in the home environment. Iyer et al. and Wang et al. stated that non-contact sensors are more comfortable for the person and provide faster results compared to contact-based sensors [17,18].

Al-Khalidi et al. suggested that non-contact respiratory monitoring methods can be divided into three groups such as optical based, radar based, thermal and thermal imaging based [19]. Since these methods have advantages and disadvantages over each other, studies are conducted with each of them in literature. In a study conducted in 2019, Chen et al. suggested a systematic framework by expressing their proposed method is feasible and effective for remote RR monitoring using face videos [20]. In other recent study, a 77 GHz FMCW radar was applied to obtain the breathing signals [18]. In another approach, Kwon et al. suggested that thermography has the potential to accurately measure RR in post-surgical patients in their study [21].

In a general article on non-contact-based methods published in 2019 [22], it was mentioned that tools like optical sensors, accelerometers and gyroscopes, radar, Wi-Fi, electromagnetic sensors, wearable technologies and acoustic sensors are used for respiratory rate estimation. The advantages and disadvantages of the tools or methods were compared in detail in that study.

Until this section, the importance of RR for health monitoring and the studies performed on RR estimation in the literature have been mentioned. In principle, most non-contact RR monitoring systems are based on obtaining signals from sensors and interpreting these signals as RR, usually using mathematical or logical methods. Although the common goal of the studies is to make the most accurate estimation, the hardware and software can be different depending on the aim. In our study, respiratory signals are obtained with radio frequency (RF) based SDR modules and machine learning is used to obtain RR from these signals. It is also concluded that non-contact RR estimation can be performed in a short time and the results can be more stable with the feature extraction and feature selection processes. In the literature, there are some studies on RR estimation with machine learning methods using radio waves [23,24]. In addition, a study expressed that radio-frequency-based non-contact health monitoring methods have become more and more attractive, especially in the home, workplace and even in clinical settings in recent years [8].

Table 2.1. *The disadvantages of contact and non-contact methods can be summarised in the table below.*

Disadvantages of Contact Based Methods	Disadvantages of Non-Contact Based Methods
Limits the mobility and comfort	Violating private life in visual systems
Not suitable for long-term and remote	Requiring daylight in visual systems
Costs	Sensitive to environment movements in mmWave, RF
Staff workload	Sensitive to posture position in mmWave, RF
Difficulty of stand-alone installation	Low accuracy compare to contact-based methods

Basically, although both methods have disadvantages, non-contact methods are preferred to overcome the deficiencies of contact methods mentioned in Table 2.1. The RF-based system used in this study will enable respiratory rate monitoring in the home environment without restricting the comfort of the patient.

Table 2.2. *Respiratory rate estimation methods.*

Methods	Tools-Sensors	References
Non-contact based	Wi-Fi sensors	[34]
	mmWave radar sensors (FMCW)	[18]
	RF sensors (SDR)	[24]
	Face videos (Photoplethysmograpy-PPG)	[20]
	Thermal camera (Thermograpy)	[21]
Contact-based	Pulse oximeters (Photoplethysmograpy-PPG)	[12]
	Electrical activities (ECG)	[9]
	Flowmeters, optic sensors, accelerometers, microphones, thermistors	[35]

Table 2.2 shows the studies on RR estimation in the literature with references. Although contact based methods are traditionally used for their robust results in hospital settings, there are also many strong alternative non-contact methods that can be used in the future.

2.2. Studies on RR Estimation with Machine Learning Models

There are many studies in the literature on RR estimation with machine learning models using SDR modules. In a study conducted in 2021, Ashleibta et al. carried out the respiratory rate monitoring and they identified some anomalies [24]. In that study, 8 different features were extracted in time domain and frequency domain from the measurements obtained using the SDR module and classification was performed with 4 different ML models. The respiratory rate of the subjects was categorized as elevated, shallow, normal. The distance between the antenna and the person was chosen as 0.4 m. Measurements were taken for 10 seconds. The 8 features Ashleibta et al. selected in their studies are shown in Table 2.3.

Table 2.3. *The 8 features Ashleibta et al. selected in their study [24].*

No	Feature	Expression
1	Normalized standard division	$Y_{sd} = \sqrt{\frac{1}{N-1}\sum_{i=1}^{N}(x_i - y_m)^2}$
2	The root mean square (RMS)	$Y_{RMS} = \sqrt{\frac{1}{N}\sum_{i=1}^{N}(x_i)^2}$
3	Peak to peak value	$Y_{ppv} = y_{max} - y_{min} \quad (i=1,2 \ldots.,N)$
4	Peak factor	$Y_p = \frac{max(x_i)}{Y_{RMS}} \quad (i = 1,2 \ldots\ldots, N)$
5	Waveform factor	$Y_w = \frac{N * Y_{RMS}}{\sum_{i=1}^{N} x_i} \quad (i = 1,2 \ldots\ldots, N)$
6	FFT	$Y_{FFT} = \sum_{n=-N}^{N} x(n)\, e^{-j\frac{2\pi nd}{N}}$
7	Spectrum probability	$Y_{SE} = \sum_{n=-N}^{N} p(d)^2$
8	Signal energy	$Y_M = \sum_{n=-N}^{N} p(d)\, ln\, p(d)$

The results obtained from their study are shown in Table 2.4 [24]. The researchers demonstrated classification accuracy with 4 different machine learning models.

Table 2.4. *The results obtained Ashleibta et al.'s study[24].*

Classification Models	Classification Accuracy %
Nearest Neighbors (KNN)	91.0105
Decision Tree (DT)	71.131
Discriminant Analysis (DA)	59.72
Naive Bayes (NB)	48.99

In other study, researchers presented a comprehensive survey of recent advances in the CSI-based sensing mechanism and illustrated drawbacks and challenges. They also presented some suggestions for the future of non-contact sensing technology [25]. They suggested that Wi-Fi CSI-based sensing technology is still immature and requires deeper investigations due to some challenges that need to be addressed in the future. Researchers listed a number of those challenges such as object interference, environment changes, unconstrained mobility and tracking two or more objects in the test area. Researchers also expressed that by applying more solutions to the current challenges, Wi-Fi CSI-based sensing techniques can be considered as the future backbone of Human–Computer Interaction (HCI) [25].

In another study [26], it was mentioned that SDR technology will have an important place on the early detection of vital signs and human health monitoring in a non-contact way. It is also pointed out the flexibility and portability of SDR technology with state-of-art machine learning algorithms in their study. Khan et al. [26] evaluated various challenges in the development of non-contact sensing platforms linked to healthcare especially including the containment of COVID-19. In their study, 18 statistical time and frequency domain features were extracted to classify the RR. Four different respiratory patterns were classified as fast, normal, slow and deep by researchers. The classification is performed by using three popular machine learning algorithms which are K-nearest neighbors (KNN), support vector machine (SVM) and decision tree (DT).

Khan et al. also suggested that their study reveals that wireless communication technologies are not only used for voice, text, videos and multimedia applications but also, they can be used in health applications. They stated that the developed platform is a viable solution for COVID-19 and non-COVID-19 scenarios, and it is also very useful in the early diagnosis of COVID-19 symptoms such as shortness of breath and dry cough [26]. The 18 features selected in Khan et al.'s study are shown in Table 2.5.

Table 2.5. *The 18 features selected in Khan et al.'s study [26].*

No	Features	Expression
1	Minimum value in data	$Y_{min} = min(x_k)$
2	Maximum value in data	$Y_{max} = max(x_k)$
3	Mean	$Y_m = \frac{1}{N}\sum_{i=1}^{N} x_k$
4	Standard deviation	$Y_{SD} = \sqrt{\frac{1}{N-1}\sum_{i=1}^{N}(x_k - Y_m)^2}$
5	Variance	$Y_V = \sum_{i=1}^{n}(x_k - Y_m)^2$
6	Root mean square	$Y_{RMS} = \sqrt{\frac{1}{N}\sum_{i=1}^{N} x_k^2}$
7	Peak to peak value	$Y_{PPV} = Y_{max} - Y_{min}$
8	Kurtosis	$Y_k = \frac{\frac{1}{N}\sum_{k=1}^{N}(\lvert x_k \rvert - Y_{MV})^4}{{Y_{RMS}}^4}$
9	Skewness	$Y_s = \frac{\frac{1}{N}\sum_{i=1}^{N}(\lvert x_k \rvert - Y_{MV})^3}{{Y_{RMS}}^3}$
10	Peak factor	$Y_p = \frac{max(x_i)}{Y_{RMS}} \quad (i = 1,2 \ldots\ldots, N)$
11	Interquartile range	$Y_{IQ} = Q_3 - Q_1$
12	Waveform factor	$Y_w = \frac{N * Y_{RMS}}{\sum_{k=1}^{N}\lvert x_i \rvert} \quad (i = 1,2 \ldots\ldots, N)$
13	FFT	$Y_{FFT} = \sum_{n=-N}^{N} x(n)\, e^{-j\frac{2\pi nd}{N}}$
14	Minimum frequency value	$Y_{fmin} = Min(Y_{FFT})$
15	Maximum frequency value	$Y_{fmax} = Max(Y_{FFT})$
16	Spectral Probability	$Y_{SP} = \frac{FFT(k)^2}{\sum_{i=-N}^{N} FFT(k)^2}$
17	Signal energy	$Y_E = \sum_{n=-N}^{N} \lvert p(k) \rvert^2$
18	Spectrum Entropy	$Y_{SE} = \sum_{i=-N}^{N} p(k)\, ln(p(k))$

In another work, to monitor different human body movements including human hand waving, coughing, and breathing, extensive experiments were conducted by Rehman et al. [27]. In this experimental setup, the dataset was collected through USRPs placed half a meter away from the participant. Each participant sat on a chair in a comfortable posture. A total of five participants performed different human body movements like hand waving, coughing, and breathing. In this work, a non-contact platform detecting the COVID-19 early, was suggested. The breathing rates were selected as 20, 10, and 28 breaths per minute for the case of normal, slow, and fast respectively [27].

In another study, Rehman et al. extracted 10 features, and RR was estimated with machine learning models [28]. The 10 features extracted by Rehman et al. in their studies are shown in Table 2.6.

Table 2.6. *The 10 features extracted Rehman et al. in their study [28].*

No	Features	Expression
1	Mean	$Y_m = \frac{1}{N}\sum_{i=1}^{N} x_k$
2	Standard deviation	$Y_{SD} = \sqrt{\frac{1}{N-1}\sum_{i=1}^{N}(x_k - Y_m)^2}$
3	Root mean square	$Y_{RMS} = \sqrt{\frac{1}{N}\sum_{i=1}^{N} x_k^2}$
4	Peak to peak value	$Y_{PPV} = Y_{max} - Y_{min}$
5	Kurtosis	$Y_k = \frac{\frac{1}{N}\sum_{k=1}^{N}(\lvert x_k\rvert - Y_{MV})^4}{{Y_{RMS}}^4}$
6	Skewness	$Y_s = \frac{\frac{1}{N}\sum_{i=1}^{N}(\lvert x_k\rvert - Y_{MV})^3}{{Y_{RMS}}^3}$
7	Shape Factor	$y_{SF} = \frac{y_{RMS}}{\frac{1}{n}\sum_{i=1}^{n}\lvert y_i\rvert}$
8	Crest Factor	$y_{CF} = \frac{max_i\lvert y_i\rvert}{y_{RMS}}$
9	Impulse Factor	$y_{IF} = \frac{max_i\lvert y_i\rvert}{y}$
10	Entropy	$y_{Ent} = \sum_{i=-n}^{n} hist(y_i)\, ln_2(hist(y_i))$

3. RESPIRATORY RATE ESTIMATION

In this section, it is described the proposed sensor and method for RR estimation. It is also explained how the data is collected and processed. Finally, RR estimation is performed using different machine learning models. The results are compared with statistical methods and other methods based on machine learning in the literature.

3.1. Theoretical Background

In this section, the importance and fundamentals of RF sensor technology, SDR modules and machine learning models employed in this study for RR estimation are discussed.

3.1.1. RF based sensing

RF based sensors are devices that use RF frequency signals to detect physical changes in any environment. An RF frequency signal is an electromagnetic wave that oscillates at a frequency universally referred to as radio frequency. Propagation of radio frequency (RF) is sensitive to the environment through their path which they travel, but it makes them very useful frequencies for sensors at the same time.

A simplified electromagnetic spectrum is shown in Figure 3.1. Here electromagnetic waves are categorized according to their frequencies. Basically, the speed of these waves is equal to the speed of light and their wavelength decreases when their frequency increases and vice versa. Therefore, depending on the frequency of the RF sensor, the sensitivity of distinguishing physical changes on the propagation path changes.

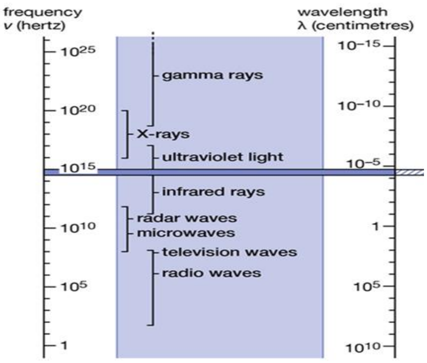

Figure 3.1. *The electromagnetic spectrum.*

In other words, radio frequency is used in many applications today according to its response to physical changes. For example, terms like Wi-Fi, Radar, RFID, Bluetooth or SDR-based that we heard before are technologies benefiting from the RF signals to communicate with the environment. RF sensors are used in many areas such as IoT applications, smart cities, autonomous systems, identification, communication, search and rescue, security. RF sensors is also an attractive technique in the field of healthcare.

3.1.2. Software defined radio (SDR)

Software-Defined Radio (SDR) "is a radio in which some or all of the physical layer functions are software defined [29]". Software defined "refers to the use of software processing within the radio system or device to implement operating functions" [29]. RF signals are generated and captured by low-cost SDR modules. The main advantage of SDR modules is that typically the center frequency, sampling rate, and bandwidth parameters of the radio waves sent from the transmitter are adjustable. Therefore, SDRs provide high flexibility and versatility to the users. They have already attracted the attention of researchers due to their advantages and affordability. In recent years, many studies have been conducted with SDR modules on topics such as gesture recognition, health monitoring, activity identification [8, 24, 25, 30, 31].

Basically, SDR modules transmit continuous-time signals to the target through a transmit antenna. Depending on some criteria like the distance and the angle between transmitter and target, the physical structure of the target and environmental conditions, the characteristics of these signals such as frequency, amplitude and phase re-emit by changing from the target. These signals re-emitted from the target are collected by a receiving antenna on the module. These signals are then converted into digital signals by signal processing methods. As a result, the digital signal is outcome of the reciprocating movements of a person's rib cage, and it includes a set of samples can be interpreted as RR. Finally, RR can be estimated from these signals with a number of methods such as machine learning.

USRP B210 used in this project is a high-performance software-defined radio (SDR) platform over a wide frequency range from 70 MHz to 6 GHz. Therefore, this platform enables us to experiment with a wide range of signals including FM and TV broadcast, cellular, Wi-Fi, and more. The USRP B210 includes a total of two receive and two transmit antennas. B210 allows you to configure and customize the hardware and software to meet the specific requirements of your application. Whether you need a solution for wireless communications, signal processing, radar, or scientific research, the USRP B210 can handle. B210s are also capable of streaming up to 56 MHz of real-time RF bandwidth. Figure 3.2 shows the USRP B210 board and its enclosure kit.

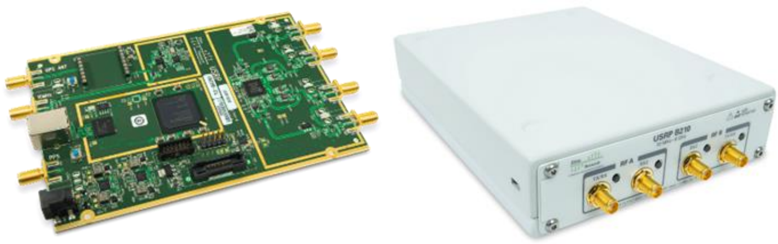

Figure 3.2. *USRP B210 (board and enclosure kit)*

3.1.3. Machine learning approach

Machine learning (ML) is the process of using mathematical models to help to learn a computer without direct interventions. In general, machine learning algorithms are used to make predictions or classification. Depending on the input data and their output, your algorithm will produce an estimate or a pattern. In other words, learning problems can be formulated as a mapping between input and output for a model. The model is trained with a set of input data and their corresponding labeled as output data and then it is evaluated in terms of the prediction accuracy. Neural networks, linear regression, logistic regression, clustering, decision trees, random forests are widely used machine learning models.

In recent years, it has been highly preferred in experiments like human activity recognition, health monitoring, face recognition, gesture recognition using RF signals with machine learning models. Since RF signal patterns are associated with human movements, it is possible to accurately recognize human movements from signal patterns using a learning-based method [8,32]. Therefore, to build an RF-based human sensing system, a link must be established between variations in the signal and human movements.

In general, the primary step of respiratory rate estimation with machine learning models is to determine the features to be applied to the input of the model. This process is defined as feature extraction in literature. The steps followed for the respiration rate estimation using RF sensors generally can be listed in the Table 3.1. This study is also processed in a flow according to the headings in this Table.

Table 3.1. *The steps followed for RR estimation.*

Sequence	Process
1	Data collection
2	Filtering process of data
3	Feature extraction (Time or frequency domain)
4	Machine learning model
5	Respiratory rate estimation

3.2. Experimental Setup and Materials

In this study, a dataset consisting of measurements collected for a previous study is used [8]. Measurements are taken in the laboratory at sitting and lying position as Figure 3.3. In experiments, ten healthy nonsmoking subjects with no history of respiratory disease are selected. The main anthropometric characteristics of the subjects are given in Table 3.2. The subjects steadily breathe at different rates range 12 breathe per minute (bpm) to 20 bpm during the experiments and a metronome which acts as the ground-truth is used to keep subjects' respiratory rate constant.

Figure 3.3. *Measurements are collected in sitting and lying positions [8].*

Table 3.2. *The anthropometric characteristics of the subjects [8].*

	Range	Mean	Median	St. Dev.
Age	23-39	31.3	32	4
Weight (kg)	70-120	79.3	75.5	17
Height (cm)	165-190	175.6	174.5	7.8

Two Universal Software Radio Peripheral (USRP) B210 modules which are deployed two sides of a chair are used as the radio transmitter and the receiver. The radio transmitter emits a continuous wave signal at 900 MHz. The transmit power of signal is adjusted as zero decibel-milliwatt (dBm) so that it doesn't have to exceed the limit specified by the Federal Communications Commission (FCC) regulations [8]. The receiver module down-samples and digitizes the RF signal to baseband for processing. After down-sampling, the sampling rate is specified as 1200 Hz which ensures the Nyquist rate criterion for obtaining the respiratory frequency. Omnidirectional antennas are used in both transmitter and receiver. The performances are obtained by using 90 records, each record is 120 seconds long.

3.3. Breathing Signal Model

Respiration is a vital process consisting of two stages which are inhalation and exhalation. While the rib cage expands during inhalation, it shrinks during exhalation. These periodic changes in the rib cage can affect the amplitude and phase of RF signals. Fig. 3.4 shows how the amplitude of the breathing signal collected from the RF sensors changes depending on whether the breathing is deep, shallow or normal. The figure also shows that human movements change the signal to a significant extent. This phenomenon shows that it is inherently difficult to obtain a reliable RR estimation with RF signals. Therefore, the person needs to pay attention not to move during the measurement.

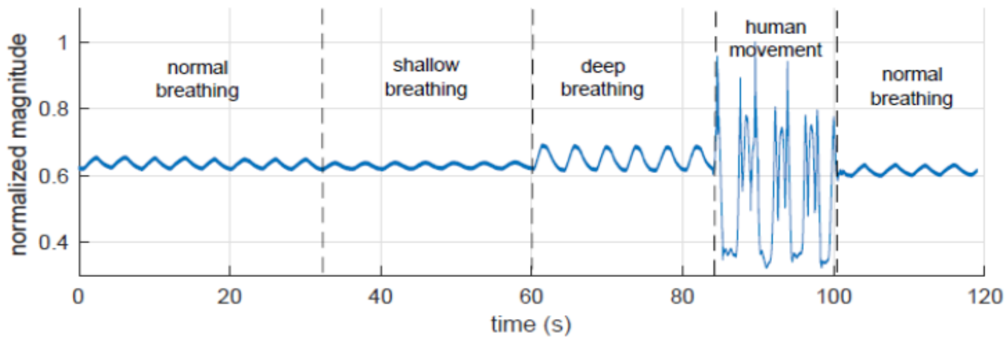

Figure 3.4. *The amplitude of the breathing signal changes depending on whether the breathing is deep, shallow or normal [8].*

In this section, the mathematical formulations of the breathing signal are considered. Depending on the chest movements of the person standing in front of the RF sensor during breathing, the phase and amplitude of the received signal changes sinusoidally. This change is expressed mathematically. When there is no movement between transmitter and receiver sensors, the magnitude of received complex baseband signal in Eq. (3.1) as the following,

$$Y_k = u_k + v_k \qquad k = 1,2, \dots \dots N \tag{3.1}$$

where k is discrete time index, and N denotes the collected sample number. u_k is the average value of the received signal. v_k is assumed as a white Gaussian random noise [8]. If there is a movement in the monitoring area, the magnitude of the received signal can be modeled as Eq. (3.2),

$$Y_k = u_k + v_k + x_k \qquad k = 1,2, \dots \dots N \tag{3.2}$$

where, x_k is the signal due to movement. x_k can be modeled as sum of the sinusoidal signals due to periodic breathing movements as Eq. (3.3),

$$x_k = \sum_{i=1}^{n} A_i \cos(2\pi f_{R_{i,k}} k T_s + \phi_i) \qquad k = 1,2, \dots \dots N \tag{3.3}$$

In Eq. (3.3), A is the amplitude, ϕ_i is the phase of the sinusoidal signal, T_s is the sampling period and i is the signal index. $f_{R_{i,k}}$ is the RR of person standing on the propagation path of the radio waves.

Figure 3.5 shows a real filtered measurement. The changes occurred in the radio channel during breathing can be seen. In the figure, the peaks of the signal represent the end point of the inhalation, and the troughs represent the end point of the exhalation. The total number of peaks or troughs gives the respiratory rate.

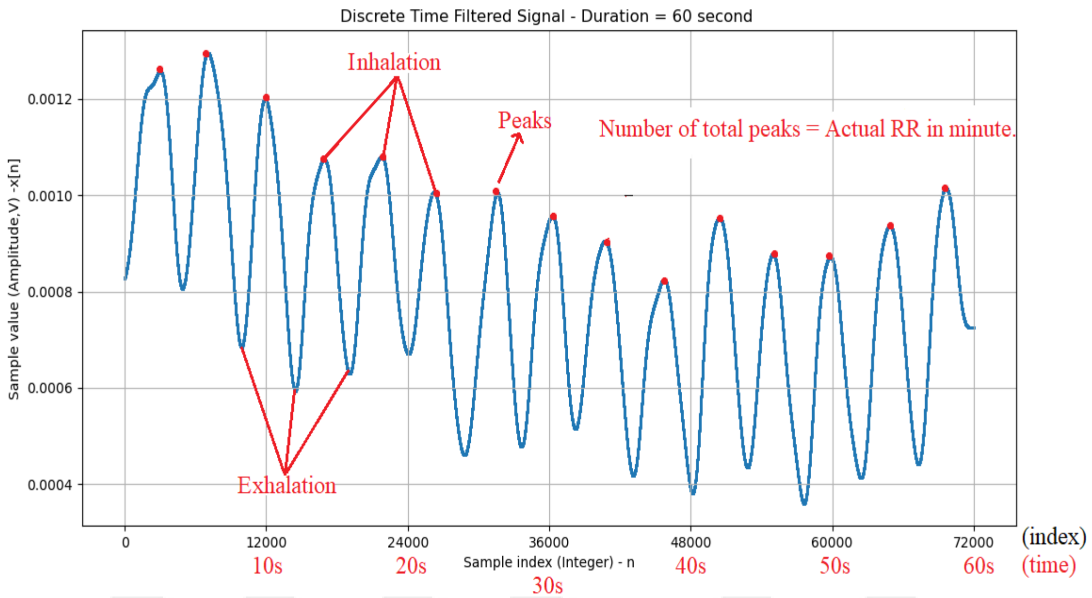

Figure 3.5. *Changes occurred in the radio channel during respiration.*

For example, the actual respiration rate of the signal in Fig. 3.5 is 15 per minute. When the graph is analyzed, it is seen that the RR estimation in 60 seconds can be obtained with high accuracy even by counting only the peaks. However, it is more complicated to estimate the RR in a short time such as 10 seconds. Because, when it is considered that there are 2 peaks in the 10-second part of the signal, the respiratory rate per minute is calculated as 12, when it is considered that there are 3 peaks, the respiratory rate per minute is calculated as 18. As a result, it is understood that it is more complicated to make a reliable RR estimation within ten seconds compared to one minute with this way. Therefore, the proposed method aims to estimate the RR with an acceptable error rate in a short observation time.

3.4. Data Processing

In this section, the data structure, data processing and filtering are discussed.

3.4.1. Data structure

The digital signal, which is the output of the SDR module, can be considered as an array or list only for a single measurement in the programming language. If the number of measurements is more than one, it can be thought of as a matrix. A representative array of 10 elements is shown in Figure 3.6. The programming language which we used allows us to find the 1st, x.th, or last element of an array, or index of the element with the smallest or largest value.

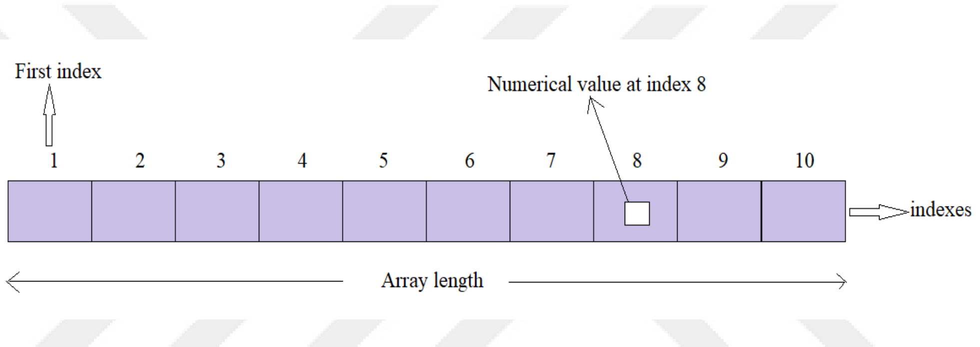

Figure 3.6. *One-dimensional array representation.*

Fig. 3.7 shows the matrix representation of the whole dataset. Since we divided the data into 10 second parts, 1080 different measurements are obtained. Each measurement consists of 12000 samples. As a result, m is 1080, n is 12000. While the rows of the matrix represent measurements, and the columns represent the indices.

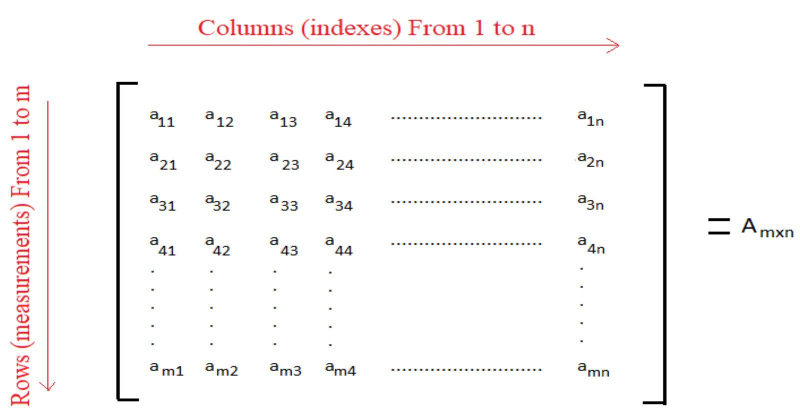

Figure 3.7. *Matrix representation of all measurements.*

Initially, the data used in this study consisted of 90 different measurements, each of them are two minutes. Each of these two-minute measurements are gradually divided into one minute, twenty seconds and ten seconds to observe the respiration rates at different durations. Fig. 3.8 shows a real one-minute original, unfiltered measurement. This signal is unfiltered, and the periodic inhalation and exhalation movements are distinguished.

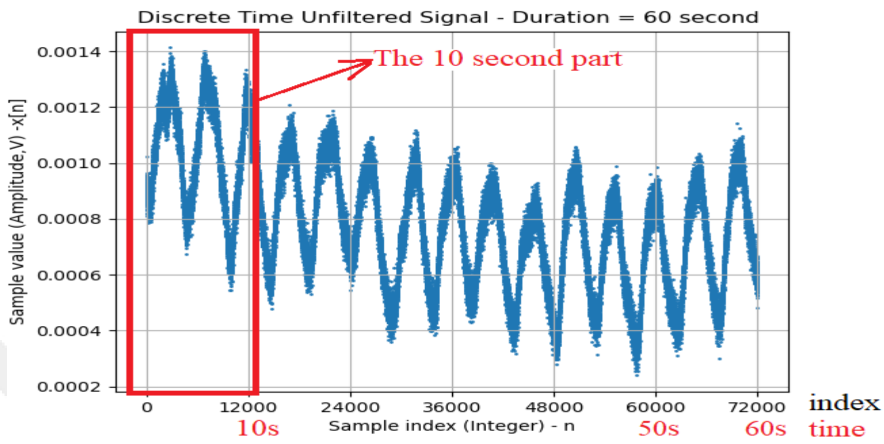

Figure 3.8. *A real one-minute measurement.*

The main motivation of the study is to attain a high accuracy RR estimation within 10 seconds. Therefore, it is focused on 10-second measurement results in this study. For example, the ten second part of the one-minute signal in Fig. 3.8 is shown in Fig. 3.9. This 10-second measurement is a digital signal consisting of 12000 samples and it can be considered as an array for the programming language. Each point in the signal in Fig. 3.9 is an element of the array.

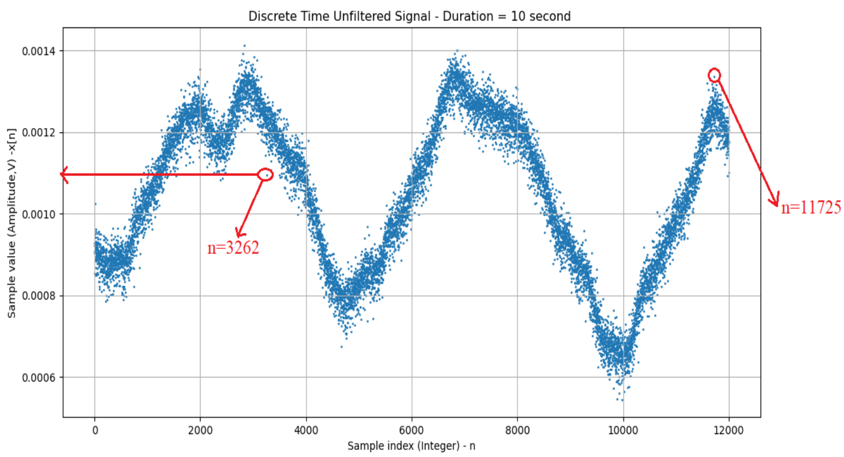

Figure 3.9. *The 10-second part of the signal indicated in Figure 3.8.*

In this 10-second signal in Fig. 3.9, it is understood that there are 12000 elements and their corresponding as amplitude values.

3.4.2. Filtering

In this study, the linear regression model is used to compare the effect of filtered and unfiltered signal on RR estimation. Linear regression models aim to predict the outcome based on a linear combination of the coefficient variables given by Eq. (3.4):

$$\hat{y} = B_0 + B_1 x_1 + B_2 x_2 + \cdots + B_m x_m \tag{3.4}$$

The values of the regression coefficients (B_0 , B_1 ,... B_m) are determined by minimizing the error rate between the real and the predicted value of y. In the formula, m denotes the total number of features.

In order to measure the efficiency of ML models for RR estimation and the effect of filtering, the mean absolute percentage error (MAPE) is used. MAPE can be modeled as Eq. (3.5)

$$MAPE = \frac{1}{n}\sum_{i=1}^{n}\left|\frac{\hat{y}_i - y_i}{y_i}\right| x100 \tag{3.5}$$

$\hat{y}_i$=Predicted value for the i^{th} data point.

y_i=Actual value for the i^{th} data point.

n =Number of observations.

It is observed that adding a filter caused a significant decrease in error rates. Filter optimization is performed, and the most suitable filter is determined to be 0.7 Hz. Since the filtering gives more reliability, all measurements are filtered. The filtered version of the signal in Fig. 3.9 is shown in Fig. 3.10. A more robust signal is obtained by removing the noise.

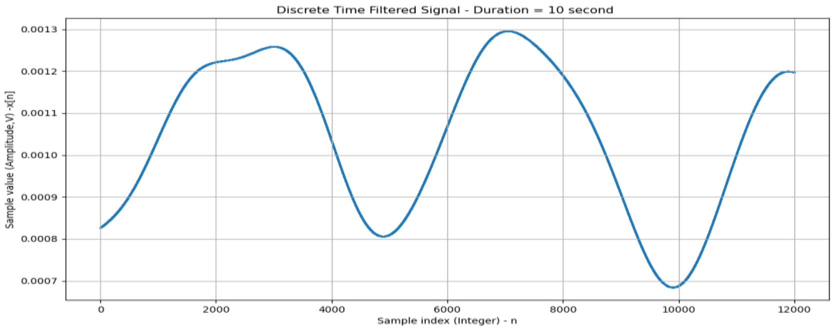

Figure 3.10. *The filtered version of the signal in Fig. 3.9.*

3.4.3. Data Enhancement

In the experimental environment of the study [8], 90 different measurements were taken, and each measurement consisted of 144000 elements covering a period of 120 seconds. In this study, we continued by converting the 120 seconds of data into 10 seconds of data in order to obtain results in a short period of time. In addition, this also allowed us to increase the amount of data available. The stages of dividing the dataset are shown in Table 3.3.

Table 3.3. *Dividing the original two-minute measurement into ten seconds.*

Time	Measurement (Row)	Array Length (Column)
120 seconds	90	144000
60 seconds	180	72000
20 seconds	540	24000
10 seconds	1080	12000

As a result of division, 90 measurements are increased to 1080 measurements and 144000 elements in each measurement are reduced to 12000. In short, a new 1080x12000 matrix is obtained when all measurements are considered. These values correspond to the values m and n in Fig. 3.7.

3.5. Proposed Method

In this section, features are extracted, and respiratory rate estimation is performed with various machine learning models.

3.5.1. Feature extraction

In this section, some features are proposed to determine the input features for the machine learning model. Some of these features are extracted from the python library named Tsfresh [33]. In total, 40 features are obtained. The creation techniques or formulas of the features are mentioned further stages.

3.5.1.1. Method-1

The aim of the method is to approximate the frequency by finding the number of samples between two peaks, two troughs and peaks and troughs in ten seconds. How the value is derived is exemplified in Fig. 3.11 for two peaks. As can be seen from Fig. 3.11, there are 12000 samples within 10 seconds. Based on that, it is concluded that the actual respiration rate per minute of the signal completing its period in every 6000 samples is 12 bpm. This would be 3600 for 20 bpm. Therefore, the RR per minute can be formulated as follows Eq. (3.6):

$$\mathrm{RR_{min}} = \frac{\text{Total number of samples in 60 seconds}}{\text{Number of samples in 1 period}} \tag{3.6}$$

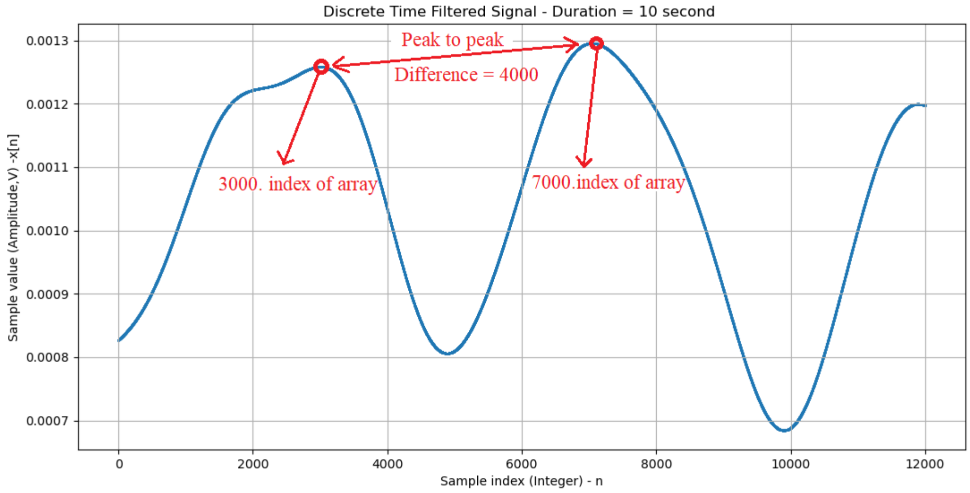

Figure 3.11. *Finding the number of samples between two peaks.*

Indexes of the 1st and 2nd peaks are found respectively and the difference between them is returned as output. The array representation of the peak determination are as follows in Fig. 3.12.

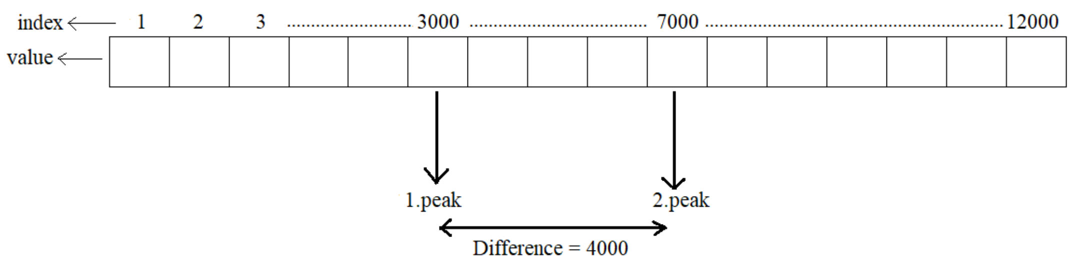

Figure 3.12. *The array representation of the peak determination.*

A part of the method written in python programming language is shown in Fig. 3.13.

```
# A is a matrix has 1080x12000 dimension matrix included of all measurement.
for k in range(1080): # 1080 measurement.
   m=-1 # variable
   n=0 # variable
   for i in range(1,12001):# 12000 element for 10 second data.
      if A[k,i]<A[k,i+1]: # Checks if the ith element of the array is less than the (i+1)th element.
         n=n+1
         if n>2000: # Has the above condition been fulfilled 2000 times.
            if A[k,i+1]>A[k,i+2]: # The first value at which the (i+1)th element is greater than the (i+2)th element.
               m=m+1
               indexofmaxelement[k,m]=i+1 # It will give the index of the maximum value respectively.
               n=0
```

Figure 3.13. *A part of the Method-1 written in python programming language.*

The stages of determining the peak points are as follows in Table 3.4.

Table 3.4. *Algorithm steps of the Method-1*

Steps	Algorithm
1	Start from the i=1st index of the array (signal).
2	Check whether the amplitude at index i of the array is less than the value at (i+1).
3	The condition in step 2 is repeated by increasing the number i by 1.
4	The condition in step 2 is expected to be fulfilled 2000 times.
5	If the condition in step 2 is fulfilled 2000 times, the first value at which the amplitude at index (i+1) is greater than the amplitude at index (i+2) is selected as maximum.

Figure 3.14 shows a representative graph of how the method is implemented. In the graph, it is understood that the amplitude of the elements in data increases continuously. This increase has to continue for 2000 index. When this condition is ensured at ith index, the amplitude of the (i+1)th index is expected to be greater than the amplitude of the (i+2)th index. In short, the amplitude of the elements must pass the decreasing.

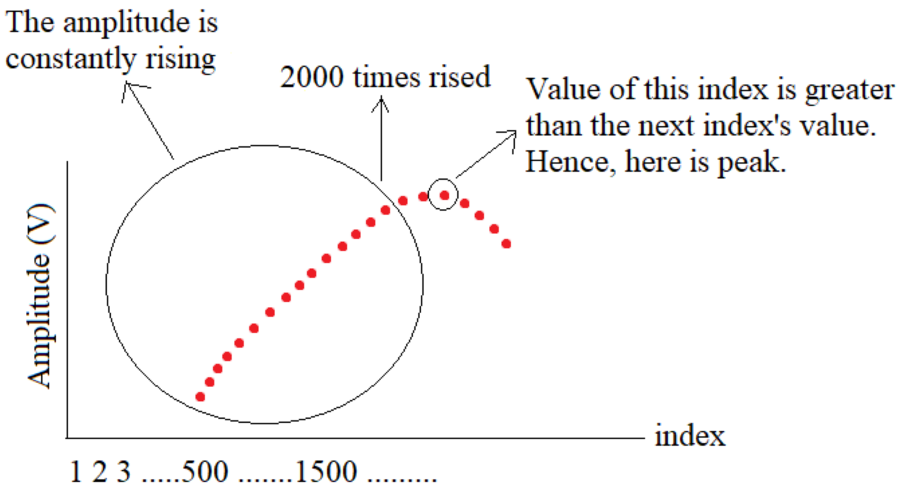

Figure 3.14. *A representative graph of how the Method-1 is implemented.*

This method is also used to find the number of samples between two troughs and peaks and troughs. In this way, 2 more features are obtained. In addition, a 4th feature is obtained by averaging these three features. All the features obtained with Method-1 are shown in Table. 3.5.

Table 3.5. *The features obtained with Method-1.*

Feature	Method	Description	Notation
1	Method-1	Number of samples between two peaks	M_{11}
2		Number of samples between two troughs	M_{12}
3		Number of samples between peaks and troughs x 2	M_{13}
4		Mean of 1,2,3. features.	M_{14}

As an example, the values obtained for only 10 measurements of the whole data are shown in Figure 3.15. The results of feature 1 (M_{11}) obtained by Method-1 were compared with the actual values. Since the number of samples in a signal with 12 bpm is 6000, it can be understood that the feature works properly.

	0	1
0	4718.67	6000
1	5911.83	6000
2	6854.5	6000
3	5845.25	6000
4	5683.5	6000
5	5836.5	6000
6	5592.25	6000
7	5638.75	6000
8	5731.25	6000
9	5911.67	6000

Figure 3.15. *Comparison of feature M_{11} with actual values.*

As can be seen from Figure 3.15, the values obtained from feature M_{11} on the left and the number of samples in a period corresponding to actual RR on the right. The example shows measurements that their actual respiratory rate is 12 per minute.

3.5.1.2. Method-2

This method aims to find the number of samples between two peaks, two troughs and peaks and troughs similar to Method-1, but with a different formulation.

As can be seen in Figure 3.16, Method-2 depends on calculating the number of samples between two peaks like Method-1. In the figure, m1, m2, m3 …., m8 are the index of maximum value in each interval. Also, it is explained in the formulation steps section how the actual peaks such as m3 and m5 are determined.

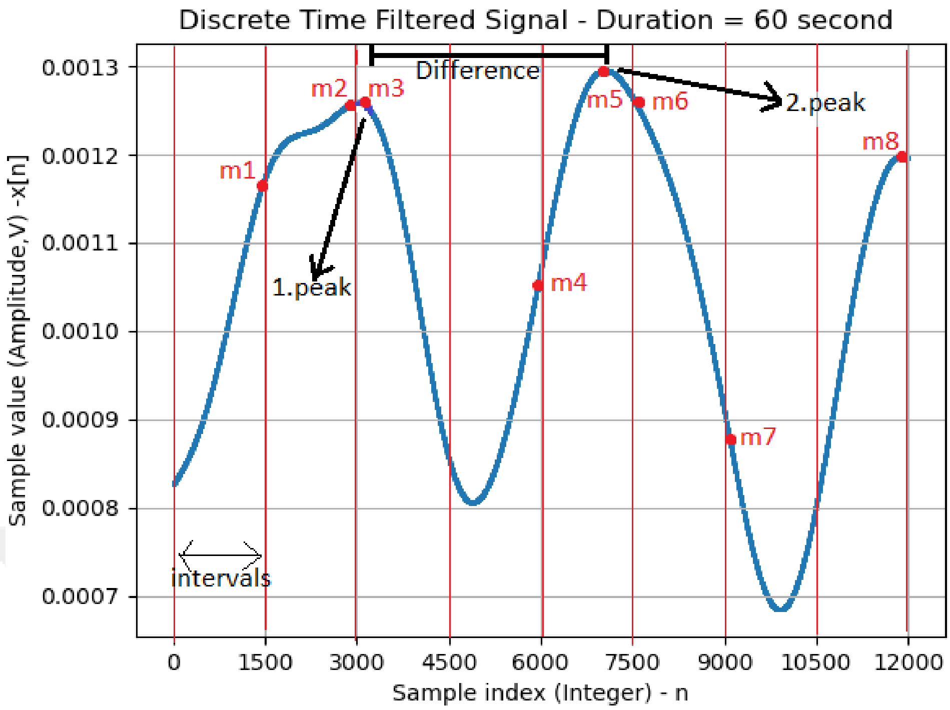

Figure 3.16. *Finding the number of samples between two peaks according to Method-2.*

The formulation steps are described below in Table 3.6.

Table 3.6. *Algorithm steps of the Method-2*

Steps	Algorithm
1	The array consisting of 12000 samples is divided into intervals containing 1500 samples.
2	The index of maximum value in each interval is found. (m1, m2, m3 …, m8)
3	If the maximum value in its own interval is greater than the maximum value in the next interval, it is selected as the peak.
4	The formulation is completed by taking the difference of the index number of the two peaks.

It is understood from the formulation that m3 and m5 are the actual peaks since they have maximum values. This method is also used to find the number of samples between two troughs and peaks and troughs. In this way, 2 more features are obtained. In addition, a 4th feature is obtained by averaging these three features.

The all features obtained with Method-2 are shown in Table. 3.7.

Table 3.7. *The features obtained with Method-2.*

Feature	Method	Description	Notation
1	Method-2	Number of samples between two peaks	M_{21}
2		Number of samples between two troughs	M_{22}
3		Number of samples between peaks and troughs x 2	M_{23}
4		Mean of 1,2,3. features.	M_{24}

In addition, 2 features are extracted from the features obtained by Method 1 and Method 2. Table 3.8 shows these features.

Table 3.8. *The features obtained with Method-1 and Method-2.*

Feature	Method	Description	Notation
1	Method-1 and Method-2	Mean of M_{14} and M_{24}	$(M_{14}+M_{24})/2$
2	Method-1 and Method-2	Ratio of M_{14} to M_{24}	M_{14}/M_{24}

Normally, two or three peaks can be seen within 10 seconds observation time. Therefore, only either second or third coefficient of the FFT is the highest. As a result, the FFT cannot give us the frequency directly but there is a linear relationship between these coefficients and respiratory rates. Therefore, the second and third coefficients of the FFT are used as a feature. Table 3.9 shows these features.

Table 3.9. *The features obtained with the power amplitude value of FFT.*

No	Description	Notation
1	Second coefficient of FFT	FFT_2
2	Third coefficient of FFT	FFT_3

3.5.1.3. Other features

Features extracted from the python package named Tsfresh or ready-made functions in the python programming language are used as other features. A total of 40 features are used in the input of the machine learning models, including 12 features from the previous section in Table 3.5, 3.7, 3.8 and 3.9 and 28 features added from other sources in Table 3.10.

Table 3.10 contains descriptions and formulas for 28 features.

Table 3.10. *Other features.*

No	Features	Notation
1	Kurtosis	$Y_k = \frac{\frac{1}{N}\sum_{k=1}^{N}(\lvert x_k\rvert - Y_{MV})^4}{{Y_{RMS}}^4}$
2	Skewness	$Y_s = \frac{\frac{1}{N}\sum_{i=1}^{N}(\lvert x_k\rvert - Y_{MV})^3}{{Y_{RMS}}^3}$
3	Signal energy	$Y_E = \sum_{n=-N}^{N}\lvert p(k)\rvert^2$
4	Count above mean	Returns the number of values in Y that are higher than the mean of Y
5	Count below mean	Returns the number of values in Y that are lower than the mean of Y
6	Last location of the maximum	Return the last location of the maximum value of Y
7	Last location of the minimum	Return the last location of the minimum value of Y
8	First location of the maximum	Return the first location of the maximum value of Y
9	First location of the minimum	Return the first location of the minimum value of Y
10	Longest strike below mean	Returns the length of the longest consecutive subsequence in Y that is smaller than the mean of Y
11	Longest strike above mean	Returns the length of the longest consecutive subsequence in Y that is bigger than the mean of Y
12	Absolute sum of changes	$\sum_{i=1}^{n-1}\lvert x_{i+1} - x_i\rvert$
13	Has duplicate min	Checks if the minimal value of x is observed more than once
14	Root mean square	$Y_{RMS} = \sqrt{\frac{1}{N}\sum_{i=1}^{N}x_k^2}$
15	Mean second derivative central	$\frac{1}{2(n-2)}\sum_{i=1}^{n-1}\frac{1}{2}(x_{i+2} - 2.x_{i+1} + x_i)$
16	Mean change	$\frac{1}{n-1}\sum_{i=1}^{n-1}(x_{i+1} - x_i)$

[Table 3.10. (Continue) Other features.]

No	Features	Notation
17	Percentage of reoccurring values to all values	Returns the percentage of values that are present in the time series more than once.
18	Benford correlation	$P(d) = \log_{10}\left(1 + \frac{1}{d}\right)$
19	Has duplicate max	Checks if the maximum value of Y is observed more than once
20	Variation coefficient	$Y_{CV} = Y_{SD}/Y_m$
21	Minimum value in data	$Y_{min} = \min(x_k)$
22	Maximum value in data	$Y_{max} = \max(x_k)$
23	Mean	$Y_m = \frac{1}{N}\sum_{i=1}^{N} x_k$
24	Standard Deviation	$Y_{SD} = \sqrt{\frac{1}{N-1}\sum_{i=1}^{N}(x_k - Y_m)^2}$
25	Variance	$Y_V = \sum_{i=1}^{n}(x_k - Y_m)^2$
26	Sum values	$Y_{sum} = \sum_{i=1}^{N} x_k$
27	FFT	$Y_{FFT} = \sum_{n=-N}^{N} x(n)\, e^{-j\frac{2\pi nd}{N}}$
28	Median	for ordered data list or array$\{x_1, x_2, \ldots . x_n\}$ $\frac{x_{\frac{n}{2}} + x_{\frac{n}{2}+1}}{2}$ if n is even

3.5.2. Machine learning models to predict RR

Machine learning models are preferred for RR estimation in the literature [24,26]. In machine learning algorithms, it is basically necessary to determine the features to be applied to the input of the model. In this study, it is used many different machine learning algorithms used previous studies in the literature. After determining 40 features to be applied to the input of the model, they are tested in different machine learning models. The values of the 40 features for each 10-second measurement are combined in a matrix to be applied to the input of the model. To be more tangible, a representation of this matrix is shown in Fig. 3.17. Here, each row indicates a 10-second measurement and each column indicates the value of the 40 features. Therefore, since the total data to be trained and tested consist of 1080 measurements that each of them are 10-second. When the value of each feature is taken for 1080 measurements. The size of input matrix is formed as 1080x40.

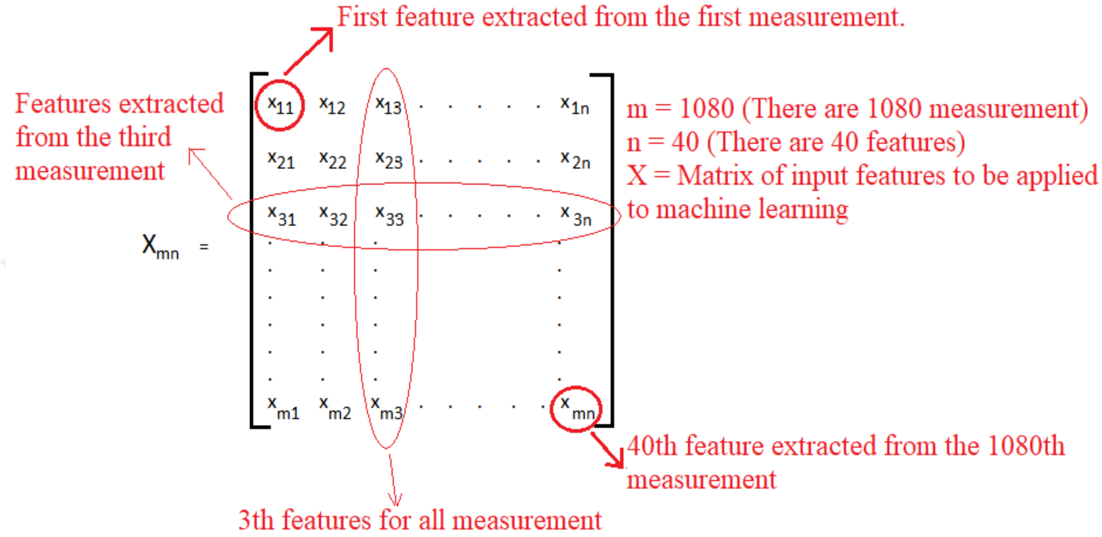

Figure 3.17. *The input matrix of machine learning model.*

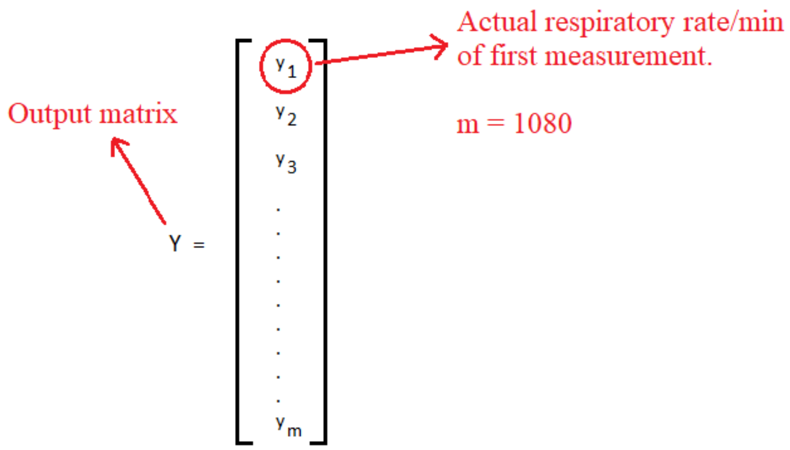

Figure 3.18. *Actual RR in minute of all measurements as a matrix.*

Fig. 3.18 shows the actual respiratory rate value of each 10-second measurement in one minute. The task of machine learning models is to make sense of the relationship between input features and output values. In this section, 1080 data are randomly sorted and divided into 80% training and 20% test. The aim here is to create a model from 80% of the data and to test the success rate of the model with 20% of the data. Ultimately, 12 different machine learning models are tested. Classification and regression types of Random Forest, Lasso, Support Vector, Decision Trees, K-nearest neighbors and Multilayer perceptron algorithms are used as machine learning models. Random Forest algorithms give the lowest MAPE value for both classification and regression because it is a good choice for structures using input features that don’t have a linear relationship between them. Since the actual respiration rates are integers, the MAPE value obtained with classification models is lower.

3.5.3. Feature selection for robust RR estimate

Among the 40 features used in the machine learning model, feature elimination or in other words feature selection is made because there could be features, they may increase the error rate in this section. In this way, more robust results are tried to be obtained. Studies are carried out to determine how many and which inputs will be applied to the machine learning model. In order to make a fair comparison with other methods performing decimal RR estimation used in different studies [8,27,36,37], we continue with the regression model. Therefore, the feature selection is implemented to the random forest regression model giving the lowest MAPE value when 40 features are used. The feature with the lowest error rate with the linear regression model is selected as the 1st feature to be applied to the model input. Then, the feature giving the lowest error rate is determined as the second feature when it is used with the first feature for random forest regression model. The error rate for 8 features is significantly reduced by continuing in this way.

3.6. Results

The results obtained from different ML models are compared. According to the results, it is seen that the Random Forest models give the most successful results both classification and regression problems. Table 3.11 shows the MAPE values of machine learning models applied in this study at section 3.5.2.

Table 3.11. *Respiratory rate estimation with different machine learning models.*

No	Approach	Method/Algorithm	MAPE (%)
1	Machine Learning Regression Algorithms	Random Forest Regression	2.73
2		Lasso Regression	4.08
3		Support Vector Regression	9.57
4		Decision Tree Regression	4.31
5		K-nearest Neighbors Regression	3.64
6		MLP Regression	4.49
7	Machine Learning Classification Algorithms	Random Forest Classification	1.69
8		Lasso Classification	4.08
9		Support Vector Classification	4.85
10		Decision Tree Classification	3.03
11		K-Nearest Neighbors Classification	3.59
12		MLP Classification	9.82

As can be seen in Table 3.11, random forest classification and random forest regression give the MAPE values of 1.69% and 2.73%, respectively. These scores are lowest for both classification and regression problems on predicting the RR.

The name Random Forest comes from the fact that the algorithm consists of many trees called decision trees. Each decision tree makes a prediction about which class the data belongs to and then it chooses the most preferred class as output. The random forest algorithm is a successful algorithm in terms of reducing the risk of overfitting and distinguishing the importance of features. For these reasons, the random forest algorithms give successful results in large datasets where there is no linear relationship between their inputs.

In the study conducted in section 3.5.3, with the 8 features in Table 3.12, the MAPE value is reduced to 2.33% from 2.73% for random forest regression. The features are meaningless when used alone and good results are obtained when they are used together. In particular, features such as count above mean, longest strike below mean and second coefficient of FFT are intended to determine the repetition time of the signal. When they used together, lower error rate is obtained.

Table 3.12. *Feature selection for robust RR estimation.*

No	Feature
1	Longest strike below mean
2	Signal energy
3	Minimum value in data
4	Mean
5	Root mean square
6	FFT_2
7	Count above mean
8	Median

Additionally, the random forest classification model is the classification model with the lowest error rate. With the 8 features in Table 3.12, the MAPE value of this model is 0.58%. Since the actual respiration rates are integers, the MAPE value is lower.

Besides machine learning models, RR estimation is also performed with different methods in literature. These methods are tried on dataset used in this study. The results are shown in Table 3.13. When the RR estimation is calculated for one-minute observation time, the MAPE value is 0.18% with the “FFT” method, 2.55% with the “peak to peak interval” method and 8.5% with the “peak detection” method. Although better results are obtained with FFT, peak to peak interval and peak detection methods within one-minute, robust results could not be obtained within a short period of 10 seconds. In signals which their observation time is ten second, there are either two peaks or three peaks. When these values are proportioned to one-minute measurements, it is understood that it will be difficult to find the other periods such as 14, 15 except for 12 and 18 with FFT and peak detection methods.

In conclusion, when the results are analyzed, it is understood that it is difficult to achieve low error rates with a single feature or method. With the machine learning model, error rates can be reduced by utilizing more than one feature. For example, there is no feature individually with a MAPE value below 3% through the 40 features used in this study. Therefore, we can attribute the high error rates of the methods proposed in previous studies to the short observation time and their inadequacy when used alone. These methods are compared with the proposed method in this study in Table 3.13.

Table 3.13. *MAPE values obtained with methods except machine learning in different studies.*

Method/Algorithm	**MAPE (%)**
Fast Fourier Transform (FFT)[37]	12.76
Peak to peak interval[36]	3.78
Peak detection [27]	17.82
Periodogram[8]	7.33
MUSIC[8]	6.66
ESPRIT[8]	5
Random Forest Regression[Proposed]	2.33

Additionally, the features used in the studies carried out on respiratory rate estimation with machine learning models in Section 2.2, are implemented to dataset used in this study. Table 3.14 shows their MAPE values. Compared to other features, a lower error rate is obtained with the features selected in this study. Here, it is thought that the results are better because there are features like longest strike below mean, count above mean and FFT_2 that directly determine the repetition time of the signal.

Table 3.14. *RR estimation with features used in the studies reviewed in Section 2.2.*

Methods	**Used Features**	**MAPE (%)**
Method in [24]	Features in Table 2.3	3.19
Method in [26]	Features in Table 2.5	2.93
Method in [28]	Features in Table 2.6	5.97
Proposed	Features in Table 3.12	2.33

4. CONCLUSIONS

In this thesis, it is demonstrated that the proposed machine learning-based method can accurately estimate respiration rate using RF signals with low error rates. By transmitting and receiving continuous wave signals through software-defined radio modules, the system captures subtle amplitude variations in the RF signals corresponding to the physical motion associated with respiration. These small variations provide information about breathing patterns, enabling precise and non-contact estimation of RR. This approach offers significant advantages over traditional techniques that require physical sensors or devices attached to the body. Furthermore, the use of SDR modules also provides flexibility, as the signal settings can be adjusted to work in different environments and with different people. The trained machine learning framework reveals the potential of RF technology to develop efficient and easy-to-use respiratory monitoring systems for healthcare applications.

Statistical methods in literature typically require observation periods that cover several signal cycles to capture the periodic nature of the signal. As a result, while they perform well over long observation periods, their accuracy tends to decrease with limited data. In contrast, the proposed method does not rely on detecting the period of the signal, which makes it less affected by short observation periods. This feature enables it to maintain high accuracy even with limited data, making it more robust and versatile for applications where long-term observation may not be possible. The proposed system is validated with real measurements from ten participants. Experiments were conducted in various positions, such as sitting and lying down, to analyze the performance of the system. The results show that the system achieves high accuracy with an error rate of 2.33% using limited data and provides a significant improvement over both statistical methods and other machine learning-based RR estimation methods in the literature.

In the proposed method, the machine learning approach involved initially extracting 40 features from the RF signaling data based on various time domain and frequency domain to comprehensively represent respiratory patterns. These features are then reduced to the eight most informative ones, improving model efficiency and focusing on key indicators of respiratory rate. Various classification and regression models are tested, and the Random Forest Regression model is selected as provides the best performance. Furthermore, this study also demonstrates the potential of integrating RF signals with machine learning models to create a low-cost, portable, and rapid respiratory monitoring system. The system's ability to provide quick RR measurements makes it suitable for applications in clinical settings and emergency scenarios. Future studies could expand the dataset to assess the system's adaptability to various demographic groups, and optimizations could be made to enable its use in real-time applications.

REFERENCES

[1] Cretikos, M.A.; Bellomo, R.; Hillman, K.; Chen, J.; Finfer, S.; Flabouris, A. Respiratory rate: The neglected vital sign. Med. J. Aust. 2008, 188, 657–659.

[2] Nicolò A, Massaroni C, Schena E, Sacchetti M. The Importance of Respiratory-Rate Monitoring: From Healthcare to Sport and Exercise. Sensors. 2020; 20(21):6396. https://doi.org/10.3390/s20216396

[3] Malasinghe, L.P., Ramzan, N. & Dahal, K. Remote patient monitoring: a comprehensive study. J Ambient Intell Human Comput 10, 57–76 (2019). https://doi.org/10.1007/s12652-017-0598-x

[4] Yunjie Fang et al 2020 J. Phys.: Conf. Ser. 1570 012029

[5] Miller DJ, Capodilupo JV, Lastella M, Sargent C, Roach GD, et al. (2020) Analyzing changes in respiratory rate to predict the risk of COVID-19 infection. PLOS ONE 15(12): e0243693. https://doi.org/10.1371/journal.pone.0243693

[6] Wuerich, C., Wichum, F., Wiede, C., & Grabmaier, A. (2021). Contactless Optical Respiration Rate Measurement for a Fast Triage of SARS-CoV-2 Patients in Hospitals. International Conference on Image Processing and Vision Engineering.

[7] Natarajan, A., Su, HW., Heneghan, C. et al. Measurement of respiratory rate using wearable devices and applications to COVID-19 detection. npj Digit. Med. 4, 136 (2021). https://doi.org/10.1038/s41746-021-00493-6

[8] C. Uysal, A. Onat and T. Filik, "Non-Contact Respiratory Rate Estimation in Real Time With Modified Joint Unscented Kalman Filter," in IEEE Access, vol. 8, pp. 99445-99457, 2020, doi: 10.1109/ACCESS.2020.2998117.

[9] Shen, CL., Huang, TH., Hsu, PC. et al. Respiratory Rate Estimation by Using ECG,Impedance, and Motion Sensing in Smart Clothing. J. Med. Biol. Eng. 37, 826–842 (2017). https://doi.org/10.1007/s40846-017-0247-z

[10]. Baker S, Xiang W, Atkinson I (2021) Determining respiratory rate from photoplethysmogram and electrocardiogram signals using respiratory quality indices and neural networks. PLoS ONE 16(4): e0249843. https://doi.org/10.1371/journal.pone.0249843

[11] W. Karlen, C. J. Brouse, E. Cooke, J. M. Ansermino, and G. A. Dumont, “Respiratory rate estimation using respiratory sinus arrhythmia from photoplethysmography,” in 2011 Annual International Conference of the IEEE Engineering in Medicine and Biology Society, pp. 1201–1204, IEEE, 2011.

[12] Iqbal, T., Elahi, A., Ganly, S. et al. Photoplethysmography-Based Respiratory Rate Estimation Algorithm for Health Monitoring Applications. J. Med. Biol. Eng. 42, 242–252 (2022). https://doi.org/10.1007/s40846-022-00700-z

[13] Teixeira E, Fonseca H, Diniz-Sousa F, Veras L, Boppre G, Oliveira J, Pinto D, Alves AJ, Barbosa A, Mendes R, Marques-Aleixo I. Wearable Devices for Physical Activity and Healthcare Monitoring in Elderly People: A Critical Review. Geriatrics (Basel). 2021 Apr 7;6(2):38. doi: 10.3390/geriatrics6020038. PMID: 33917104; PMCID: PMC8167657.

[14] Shuzan MNI, Chowdhury MH, Chowdhury MEH, Murugappan M, Hoque Bhuiyan E, Arslane Ayari M, Khandakar A. Machine Learning-Based Respiration Rate and Blood Oxygen Saturation Estimation Using Photoplethysmogram Signals. Bioengineering.2023; 10(2):167. https://doi.org/10.3390/bioengineering10020167

[15] Li, Y., Liu, C., Zou, H., Che, L., Sun, P., Yan, J., ... & Wang, Z. L. (2023). Integrated wearable smart sensor system for real-time multi-parameter respiration health monitoring. Cell Reports Physical Science, 4(1).

[16] Argüello-Prada EJ, Marcillo Ibarra KD, Díaz Jiménez KL. The use of successive systolic differences in photoplethysmographic (PPG) signals for respiratory rate estimation.Heliyon.2024Feb8;10(4):e26036.doi: 10.1016/j.heliyon.2024.e26036. PMID: 38370197; PMCID: PMC10869914.

[17] Iyer S, Zhao L, Mohan MP, Jimeno J, Siyal MY, Alphones A, Karim MF. Mm Wave Radar-Based Vital Signs Monitoring and Arrhythmia Detection Using MachineLearning. Sensors. 2022; 22(9):3106. https://doi.org/10.3390/s22093106

[18] Wang Y, Wang W, Zhou M, Ren A, Tian Z. Remote Monitoring of Human Vital Signs Based on 77-GHz mm-Wave FMCW Radar. Sensors. 2020; 20(10):2999. https://doi.org/10.3390/s20102999

[19] Farah Q Al-Khalidi, Reza Saatchi, Derek Burke, Heather E Elphick, Stephen Tan. Respiration Rate Monitoring Methods: A Review. Pediatric Pulmonology, 2011, 46 (6), pp.523. 10.1002/ppul.21416.hal-00612787

[20] M. Chen, Q. Zhu, H. Zhang, M. Wu and Q. Wang, "Respiratory Rate Estimation from Face Videos," 2019 IEEE EMBS International Conference on Biomedical & Health Informatics (BHI), Chicago, IL, USA, 2019, pp. 1-4, doi: 10.1109/BHI.2019.8834499.

[21] Kwon, HM., Ikeda, K., Kim, SH. et al. Non-contact thermography-based respiratory rate monitoring in a post-anesthetic care unit. J Clin Monit Comput 35, 1291–1297 (2021). https://doi.org/10.1007/s10877-020-00595-8

[22] Liu H, Allen J, Zheng D, Chen F. Recent development of respiratory rate measurement technologies. Physiol Meas. 2019 Aug 2;40(7):07TR01. doi: 10.1088/1361-6579/ab299e. PMID: 31195383.

[23] Mosleh S, Coder JB, Scully CG, Forsyth K, Al Kalaa MO. Monitoring Respiratory Motion With Wi-Fi CSI: Characterizing Performance and the BreatheSmart Algorithm. IEEE Access. 2022;10:131932-131951. doi: 10.1109/access.2022.3230003. Epub 2022 Dec 22. PMID: 36632174; PMCID: PMC9830631.

[24] A. M. Ashleibta, Q. H. Abbasi, S. A. Shah, M. A. Khalid, N. A. AbuAli and M. A. Imran, "Non-Invasive RF Sensing for Detecting Breathing Abnormalities Using Software Defined Radios," in IEEE Sensors Journal, vol. 21, no. 4, pp. 5111-5118, 15 Feb.15, 2021, doi: 10.1109/JSEN.2020.3035960.

[25] Al-qaness MAA, Abd Elaziz M, Kim S, Ewees AA, Abbasi AA, Alhaj YA, Hawbani A. Channel State Information from Pure Communication to Sense and Track Human Motion: A Survey. Sensors. 2019; 19(15):3329. https://doi.org/10.3390/s19153329

[26] Khan, M.B.; Rehman, M.; Mustafa, A.; Shah, R.A.; Yang, X. Intelligent Non-Contact Sensing for Connected Health Using Software Defined Radio Technology. Electronics 2021, 10, 1558. https://doi.org/ 10.3390/electronics10131558

[27] Rehman M, Shah RA, Khan MB, Ali NAA, Alotaibi AA, Althobaiti T, Ramzan N, Shah SA, Yang X, Alomainy A, Imran MA, Abbasi QH. Contactless Small-Scale Movement Monitoring System Using Software Defined Radio for Early Diagnosis of COVID-19. IEEE Sens J. 2021 May 4;21(15):17180-17188. doi: 10.1109/JSEN.2021.3077530. PMID: 35789227; PMCID: PMC8791440.

[28] Rehman, M.; Shah, R.A.; Ali, N.A.A.; Khan, M.B.; Shah, S.A.; Alomainy, A.; Hayajneh, M.; Yang, X.; Imran, M.A.; Abbasi, Q.H. Enhancing System Performance through Objective Feature Scoring of Multiple Persons' Breathing Using Non-Contact RF Approach. Sensors 2023, 23, 1251. https://doi.org/ 10.3390/s23031251

[29] Software-Defined Radio for Engineers, by Travis F. Collins, Robin Getz, Di Pu, and Alexander M. Wyglinski, 2018, ISBN-13: 978-1-63081-457-1.

[30] Zhang, O., & Srinivasan, K. (2016). Mudra: User-friendly Fine-grained Gesture Recognition using WiFi Signals. Proceedings of the 12th International on Conference on emerging Networking EXperiments and Technologies.

[31] Xu Y, Amineh RK, Dong Z, Li F, Kirton K, Kohler M. Software Defined Radio-Based Wireless Sensing System. Sensors. 2022; 22(17):6455. https://doi.org/10.3390/s22176455

[32] https://scikit-learn.org/stable/modules/neural_networks_supervised.html

[33] https://tsfresh.readthedocs.io/en/latest/text/list_of_features.html

[34] Kontou, P, Ben Smida, S & Anagnostou, DE 2024, 'Contactless Respiration Monitoring using Wi-Fi and Artificial Neural Network Detection Method', IEEE Journal of Biomedical and Health Informatics , vol. 28, no. 3, pp. 1297-1308. https://doi.org/10.1109/JBHI.2023.3337001

[35] Massaroni C, Nicolò A, Lo Presti D, Sacchetti M, Silvestri S, Schena E. Contact-Based Methods for Measuring Respiratory Rate. Sensors (Basel). 2019 Feb 21;19(4):908. doi: 10.3390/s19040908. PMID: 30795595; PMCID: PMC6413190.

[36] Park, Jinsoo & Hong, Kwangseok. (2023). Facial Video-Based Robust Measurement of Respiratory Rates in Various Environmental Conditions. Journal of Sensors. 2023. 1-16. 10.1155/2023/9207750.

[37] Mosleh S, Coder JB, Scully CG, Forsyth K, Al Kalaa MO. Monitoring Respiratory Motion With Wi-Fi CSI: Characterizing Performance and the BreatheSmart Algorithm. IEEE Access. 2022;10:131932-131951. doi: 10.1109/access.2022.3230003. Epub 2022 Dec 22. PMID: 36632174; PMCID: PMC9830631.

CURRICULUM VITAE

ORCID ID: 0009-0007-9891-5928

Name Surname :**Ufuk KİRAZCI**

Foreign Language :**English**

Education and Professional Background:

- 2010-2015, Suleyman Demirel University, Engineering Faculty, Electrical and Electronic Engineer
- 2020-Present, Engineer, Turkey Radio Television Company.
- 2021-Present, Eskisehir Technical University, Electrical and Electronic Engineering Department, Institute of Graduate Programs